Proceedings of ASME Turbo Expo 2003
Power for Land, Sea, and Air
June 16–19, 2003, Atlanta, Georgia, USA

GT2003-38454

A NUMERICAL INVESTIGATION OF AEROACOUSTIC FAN BLADE FLUTTER

X. Wu, M. Vahdati, A. I. Sayma and M. Imregun

Imperial College of Science, Technology and Medicine
Mechanical Engineering Department
London SW7 2BX, UK

ABSTRACT

This paper reports the results of an ongoing research effort to explain the underlying mechanisms for aeroacoustic fan blade flutter. Using a 3D integrated aeroelasticity method and a single passage blade model that included a representation of the intake duct, the pressure rise vs. mass flow characteristic of a fan assembly was obtained for the 60%-80% speed range. A novel feature was the use of a downstream variable-area nozzle, an approach that allowed the determination of the stall boundary with good accuracy. The flutter stability was predicted for the 2 nodal diameter assembly mode arising from the first blade flap mode. The flutter margin at 64% speed was predicted to drop sharply and the instability was found to be independent of stall effects. On the other hand, the flutter instability at 74% speed was found to be driven by flow separation. Further post-processing of the results at 64% speed indicated significant unsteady pressure amplitude build-up inside the intake at the flutter condition, thus highlighting the link between the acoustic properties of the intake duct and fan blade flutter.

1. INTRODUCTION

Vibration is a universal engineering problem and most components, which are subjected to high-speed airflow, are also susceptible to self-excited vibration, or flutter. In turbomachinery applications, flutter is usually associated with fan blades, though other compressor and low-pressure turbine blades may also suffer from such instabilities. Indeed, there is a long history of flutter problems in the design of aero-engine fans. A review of turbomachinery aeroelasticity is given by Marshall & Imregun (1996) where flutter prediction methods are described in some detail. These range from uncoupled methods which treat the fluid and the structure as two distinct media (Kielb & Ramsey 1989) to fully-coupled time-domain analyses where boundary conditions are exchanged between the two domains at each time step (Vahdati & Imregun 1996). A full literature survey is well beyond the scope of this paper and emphasis will be placed on the actual flutter mechanism rather than prediction methodologies.

In the main, fan flutter is observed in 1 to 6 forward travelling nodal diameter assembly modes, the blades usually vibrating in their first flap mode. The worst condition, for which the stability margin from the working line is smallest, typically occurs between 60% and 80% speeds. Within that interval, the flutter stability may be reduced sharply for specific narrow speed ranges, hence the term "flutter bite". Over the last ten years, measurements on aero-engine test rigs and theoretical considerations have led to the hypothesis that flutter bite may be linked to the acoustic properties of the intake duct. It has been postulated that the variation in the cross-sectional area of the duct may cause acoustic waves from the fan to be cut-off at the intake throat, the trapped energy leading to an acoustic resonance and to greater susceptibility to fan blade flutter. Chew et al (1998) were amongst the first who studied the flutter behaviour of a typical industrial configuration, a 26-bladed fan assembly, using a large-scale time-domain numerical model which included an axisymmetric intake duct representation. They showed that the intake was instrumental flutter initiation modes and they noted considerable acoustic activity within the intake. The work was extended by Vahdati et al. (2002) who studied the same fan assembly for two different duct configurations, namely a test rig intake and a flight intake (**Fig. 1**). Using an inviscid unsteady flow representation where the viscous losses were based on their steady-state counterparts, they were able to predict not only the flutter bite behaviour but also to link it to intake duct acoustics. They demonstrated that the flutter behaviour of the same basic fan assembly changed markedly when used with two different intake ducts (**Fig. 2**). Both the duct length and the duct radial profile were seen to influence the flutter behaviour.

The aim of this paper is to extend the work of Vahdati et al. (2002) by improving the modeling level on three important areas. First, the unsteady flow will be represented in a viscous fashion. Second, the discretization quality will be improved by extending the grid downstream and by using a much finer resolution. Third, a variable nozzle will be used as a novel downstream boundary condition to allow the pressure behind the fan blade to adjust automatically. It should be noted that the static pressure at the nozzle exit is set to the local ambient pressure, while the characteristic line is obtained by changing the nozzle area. Such an approach allows the determination of a more accurate fan characteristic and, more significantly, the stall boundary is reached without any numerical problems. The previous analysis by Vahdati et al. (2002) was conducted along a higher working line than the nominal, but sufficiently away from stall to avoid numerical difficulties associated with the stall boundary. The current analysis has no such limitations and hence it is, for the first time, possible to distinguish between stall and flutter mechanisms. Finally, it should be noted that the flutter analysis could be conducted using the single passage model of Vahdati et al. (2001). Such an approach has two advantages. First, it allows the use of a very fine mesh to capture the acoustic activity. Second, the post-processing of the unsteady flow results is much easier since only one vibration mode is considered at a time. This approach was used partly in the present analysis.

2. THEORETICAL BACKGROUND

The details of the Imperial College aeroelasticity code used in this study have already been described by Sayma et al. (2000a & 2000b). The single passage flutter methodology is described by Vahdati et al. (2001) who compared results from several approaches against measurements obtained from an actual flutter test rig. The development of the variable nozzle boundary condition and its application to a typical fan assembly have been reported by Vahdati et al. (2003). A brief overview will be given below for the sake of completeness but the interested reader should consult the above references.

The flow model is based on Reynolds-averaged Navier-Stokes equations with Baldwin-Barth, or Spalart-Allmaras one-equation turbulence models. The flow domain is described using general unstructured grids of 3D elements such as tetrahedra, hexahedra and wedges, a feature that offers great flexibility for modelling complex shapes. The individual elements can have any number of boundary faces and the flow variables are stored at the vertices. The numerical scheme is second-order accurate in space for tetrahedral meshes. The time stepping is done in an implicit fashion and hence very large CFL numbers can be used without creating numerical instabilities in the solution algorithm. The so-called "dual time stepping" is used for unsteady calculations. The time accuracy is guaranteed by the outer iteration level where the time-step is fixed throughout the solution domain, while the inner iterations can be performed using traditional acceleration techniques such as local time stepping and residual smoothing.

The structural part of the code uses a modal model obtained from a 3D finite element representation. It is inherently assumed that the structural behavior is linear and that the amplitude is small compared to the blade chord. The mode shapes are interpolated onto the fluid mesh and hence velocities and displacements can be calculated without interpolation during the coupled motion. The equations are advanced in time using the Newmark-β method, which is unconditionally stable. During the course of the aeroelastic computations, the mesh is moved dynamically at each time step in order to adapt to the instantaneous shape and position of the deformed structure. The information exchange between the two domains is therefore achieved via pressures and displacements.

The flutter analysis is performed using a single-passage model, which has an arbitrary inter-blade phase angle capability. The formulation tracks the periodicity of the blade motion by storing the flow variables in time and by using these to impose a given inter-blade phase angle (IBPA). Another important feature is that the viscous representation of the flow, which is required both to capture the shock position and strength accurately and to simulate the behaviour near the stall boundary. The flutter solution procedure begins by prescribing an aeroelastic motion in a given nodal diameter mode by specifying the associated natural frequency and the amplitude of vibration in that mode. The computation is continued until a periodic flow solution in time is obtained. Frequency changes due to aerodynamic effects are ignored and only one mode at a time can be analysed, thus ignoring any potential coupling between the modes. The flutter stability is inferred from the (negative or positive) work done by the generalised aerodynamic force on the blade. In other words, the product of modal velocity and modal force is integrated over a vibration cycle. Negative work implies transfer of energy from the blade to the flow, and positive work done indicates a transfer of energy from the flow to the blade. The former case is stable; the latter case is unstable if the blade cannot dissipate the additional energy by some mechanical damping mechanism. An alternative solution method, available in the same solver, is the modelling of the whole fan assembly, an approach that allows the simultaneous consideration of all vibration modes. Such a route is not pursued here because the study is focussed on a small number of nodal diameter assembly modes arising from the blade 1F mode. Furthermore, it is much easier to post-process the acoustic waves when there is only one mode of vibration.

The use of a variable-nozzle downstream boundary condition allows to consider any point on a given speed characteristic by simply modifying the nozzle area, the actual boundary conditions being set to atmospheric ones in all cases. Indeed, when the static pressure is fixed downstream the fan the flow is stable at lower working lines but numerical difficulties occur at higher working lines. It is well known that

rigid boundary conditions, based on imposing given exit pressure distributions close to the fan, are not suitable for numerical studies for which the fan is operating near stall. In such cases, the pressure profiles downstream the fan are neither known nor fixed. Furthermore, at high working lines, the flow becomes genuinely unsteady near the stall boundary, and the imposition of a fixed exit static pressure at a domain boundary close to the blade is likely to result in numerical instabilities, the so-called "numerical stall". The new approach makes the boundary conditions "less stiff" and provides a powerful natural boundary condition for stall studies. Moreover, since the aim is to simulate, as much as possible, engine and rig tests, nozzle area changes can be used to move to any point on the compressor characteristic. The application of such a methodology for computing a part-speed characteristic of a fan blade will be presented in the next section.

3. CASE STUDY

The case study is for a development-engine fan assembly with 26 blades. The aims are threefold:

(i) To obtain a detailed characteristic for the 60%-80% speed range using the variable nozzle method,

(ii) To determine the flutter boundary, including the so-called flutter bite phenomenon, for 2 the nodal diameter mode and,

(iii) To attempt to explain the flutter bite mechanism.

3.1 Determination of the fan characteristic

As mentioned earlier, the steady-state computations were conducted using a single-passage model that included both an intake and a downstream variable nozzle (**Fig. 3**). Atmospheric total temperature, total pressure and zero flow angles were prescribed upstream while atmospheric static pressure was imposed at the nozzle exit. The 60%-80% speed range was covered in 2% increments and about 5 points were considered for each speed characteristic. It is important to note that both the inlet and outlet boundary conditions remain the same for all the points. Different points on the speed characteristic are obtained by changing the area of the exit nozzle, the path from choke to stall requiring an area decrease and vice-versa. An important feature of current flutter computations is the extension of the domain to avoid reflections from the boundary caused by finite amplitude waves. Given the difficulties of devising and applying 3D non-reflecting boundary conditions for unsteady flows, a practical solution is to extend and coarsen the grid to move the boundary further away from the source. However, it is recognized that this particular approach has limitations since there is no guarantee that all waves will be absorbed with such a treatment. Hence, the development of full 3D non-reflecting boundary conditions for unsteady flows is highly desirable.

When conducting flutter studies, it is important to have the blade in its correct running position. Indeed, large blades may deform by a significant amount from their manufactured shape under the combined effect of centrifugal (CF) loads and gas pressure, a phenomenon known as "untwist". In the steady-state single-passage calculations, the blade untwist is taken into account by using the blade vibration modes that are obtained from a finite element model at the corresponding speed. Under the steady-state pressure distribution, the CF-corrected mode shapes settle to their running position about which the final flow solution is obtained.

11 steady-state solutions along the working line, corresponding to 11 speeds between 60% and 80%, are shown in **Fig. 4** in the form of Mach number contours near the tip region. As expected, the passage shock is close to the leading edge at low speeds while it moves further back at higher speeds. At higher speeds, the shock is seen to propagate into the intake duct up to 76% speed, above which, the propagation is reduced by shock weakening due to interaction with leading edge expansion. From a noise generation viewpoint, the first blade-passing harmonic will give rise to a 26^{th} circumferential mode since there are 26 blades. From a flutter viewpoint, the fan assembly vibration in low nodal diameter modes, here second and third nodal diameters, creates the unsteady pressure disturbance that might interact with duct acoustics.

Using the variable nozzle boundary condition, it was possible to obtain a hysteresis loop, characteristic of fan behavior at incipient stall or surge (**Fig. 5**). Once the fan is operating near the stall boundary, the flow is no longer steady since both the mass flow and the pressure ratio begin to vary with time. Provided the computations are conducted in a time-accurate fashion, the pressure rise across the fan will adjust itself automatically. Starting from a drop in the mass flow, the hysteresis loop can be described as follows. As the mass flow decreases, the pressure rise also decreases and the system moves to a lower working line. In this new operating condition at a reduced pressure ratio, the mass flow increases and the fan tries to move to its original working line. This causes an increase in the pressure ratio and the mass flow drops. The hysteresis characteristic in **Fig. 5** was determined from the pressure and mass flow time histories of the time-accurate calculations at stall. The center of area of the hysteresis loop may be considered to be the "equivalent" stall point and this definition was used to produce the fan map of **Fig. 6**. A comparison of the working line with the stall line indicates that, as expected, there is more stall margin at higher speeds than lower speeds.

3.2 Determination of the flutter bite

As mentioned earlier, the flutter analysis was conducted using the single-passage analysis method, which considers only one vibration mode at a time. Only 2 nodal diameter mode, arising from blade mode 1F, was considered. The 1F mode shape is plotted in **Fig. 7** where the contour levels indicate the amount of vibratory motion, with the tip section exhibiting the largest response. Such a simplified single-passage analysis method is possible because previous experience indicates that fan

assembly flutter occurs, in the main, for the blade 1F mode and for low nodal diameter modes.

As in rig tests, a series of flutter analyses was conducted by approaching the stall line on a given speed characteristic. For each speed at least two points must be considered to get the respective damping values. The point with negative damping is obtained by linear interpolation or extrapolation. The flutter boundary was defined by joining the points at which the analysis yielded negative aerodynamic damping. The results are summarized in **Figs. 8** for 2 nodal diameter mode. The trend of the predicted flutter boundary exhibits the flutter bite behavior, which has been observed during rig tests of development engines. There are sharp stability drops for very narrow speed ranges, namely around 64% and 74%, some occurring very near the working line. As will be discussed in the next section, the flutter bite phenomenon is believed to be driven by the intake acoustics.

3.3 Explanation of the flutter mechanism

The two flutter regions, occurring around 64% and 74% speeds, will now be investigated in more detail. The flow separation on the blade surface, characterized by negative axial velocity, is plotted in **Fig. 9** for both cases. There is a large separation region, located at 70% height, for the 74% speed case. Such a finding seems to suggest that flutter is driven by flow separation at this speed. On the other hand, the flutter mechanism must be different at 64% speed, since there is no evidence of flow separation, even near the high-working line where the flow remains fully attached (**Fig. 9b**).

To investigate the flutter behaviour for 64% speed case, three pressure monitoring points, labelled P1, P2 and P3 in **Fig. 3**, were selected along the flight intake. The steady increase in the pressure amplitude at each point can be seen from **Fig. 10**. The pressure build-up in the duct suggests that a significant amount of energy is trapped inside the intake, as the amplitude of the disturbance close to fan face increases every cycle, thus providing a potential mechanism for flutter instability. It is likely that such a case will occur when the pressure perturbation from the fan face will match an acoustic mode of the intake, a phenomenon of a resonance-like mechanism, driven by a frequency and mode shape match.

To investigate such a possible match between the intake duct acoustics and the perturbation at the fan face, it was decided to study the intake-alone behaviour by imposing a 2 nodal diameter pressure variation at different rotational speeds. At this stage, it was realised that an intake duct, with an extended grid covering the entire 3D domain around the intake will represent the physical behaviour of the intake duct acoustics better than a long cylindrical extension used in the previous flutter analyses. The frequency of the rotating fan perturbation can be computed from $\omega = \omega_b + N \times \Omega$, where ω_b is the assembly vibration frequency, N is the nodal diameter number and Ω is the rotation speed. The resulting velocity variation was monitored at the intake exit (fan face) and the duct impedance, defined as the ratio of pressure to velocity variation, is plotted in **Fig. 11**. It is clearly seen that the duct has an acoustic mode around 110 Hz, which is believed to be responsible for the flutter bite at 64% speed. There is no acoustic mode for the 74% speed, confirming that flutter at this speed is driven by flow separation. To investigate the acoustic behaviour of the intake further, the intake-alone pressure contours due to a rotating 2 nodal diameter pressure perturbation are plotted in **Fig 12** for various speeds. It is seen from **Fig. 12** that the acoustic mode is just cut-off around 110 Hz, a condition that matches the intake-alone acoustic mode of **Fig. 9**,

CONCLUDING REMARKS

The flutter instability seems to have at least two different mechanisms, namely flow separation and pressure build-up due to intake acoustics. It is likely that these two mechanisms will be linked at some speeds.

During rig testing of development engines, sudden reductions in flutter margin may occur for very narrow speed ranges. It has been possible to simulate such observed behaviour using an integrated aeroelasticity model. The predicted “flutter bite” consists of several sharp drops, each corresponding to an unsteady pressure build-up inside the intake. The maximum response is likely to occur when the pressure perturbation due to fan rotation and blade vibration matches, both in frequency and shape, an acoustic mode of the intake. During the numerical simulations, inherent mechanical damping was assumed to be zero and, although its inclusion will improve the overall stability, the general trend is likely to remain the same.

It was shown that using a downstream variable-area nozzle was able to provide a superior boundary condition over the standard static exit pressure boundary condition.

It is concluded that a full description of aeroacoustic flutter instability needs to include an intake model. In the general case, there may be multi-harmonics in the unsteady pressure field and hence a whole-annulus model may be more appropriate to study the possibility of modal interactions during flutter. It also may be necessary to properly account for the influence of neighbouring blade rows in compressor flutter cases. In any case, the flutter margin may well be higher for straight test rig intakes than for flight intakes since the presence of throat and droop may increase the likelihood of acoustic reflections.

ACKNOWLEDGMENTS

The authors would like to thank the UK Engineering and Physical Sciences Research Council (EPSRC) for funding the work. They also thank Rolls-Royce plc for providing some of the data. They gratefully acknowledge the contribution of their colleagues Mr. C. Freeman and Dr. J. G. Marshall in the form of many useful discussions.

REFERENCES

Bakhle, M. A., Reddy, R. & Keith, T. H. 1992. Time domain flutter analysis using a potential solver. AIAA Journal 30, 163-173

Chew, J. W., Vahdati, M. & Imregun, M. 1998. Predicted influence of intake acoustics upon part-speed flutter. ASME paper 98-GT-558.

Guruswamy, G. P. & Goorjian, P. M. 1988. Unsteady transonic aerodynamics and aeroelastic calculations at low supersonic freestreams. Journal of Aircraft 25, 955-967

Kielb, R. E. & Ramsey, J. K. 1989 Flutter of a fan in supersonic axial flow. Journal of Turbomachinery 111, 461-71

Marshall, J. G. & Imregun, M. 1996. A review of aeroelasticity methods with emphasis on turbomachinery applications. J Fluids & Structures 10, 237-267

Sayma, A. I., Vahdati, M. & Imregun, M. 2000a, Multi-stage whole-annulus forced response predictions using an integrated non-linear analysis technique – Part I: Numerical Model. Journal of Fluids and Structures 14(1), 87-101

Sayma, A. I., Vahdati, M., Sbardella, L. & Imregun, M. 2000b Modelling of 3D viscous compressible turbomachinery flows using unstructured hybrid grids. AIAA Journal 38(6), 945-954

Vahdati, M. & Imregun, M. 1996 A non-linear integrated aeroelasticity analysis of a fan blade using unstructured dynamic meshes. Journal of Mechanical Engineering Science, Part C, 210, 549-563

Vahdati, M., Sayma, A. I., Marshall, J. G. & Imregun, M. 2001 Mechanisms and prediction methods for fan blade stall flutter. AIAA Journal of Propulsion & Power 17(5), 1100-1108

Vahdati, M., Sayma, A. I., Breard, C. & Imregun, M. 2002 Computational study of intake duct effects on fan flutter stability. AIAA Journal 40(3), 408-418

M. Vahdati, A. I. Sayma, C. Freeman & M. Imregun 2003 On the use of atmospheric boundary conditions for axial-flow compressor stall simulations. Submitted to the Journal of Turbomachinery.

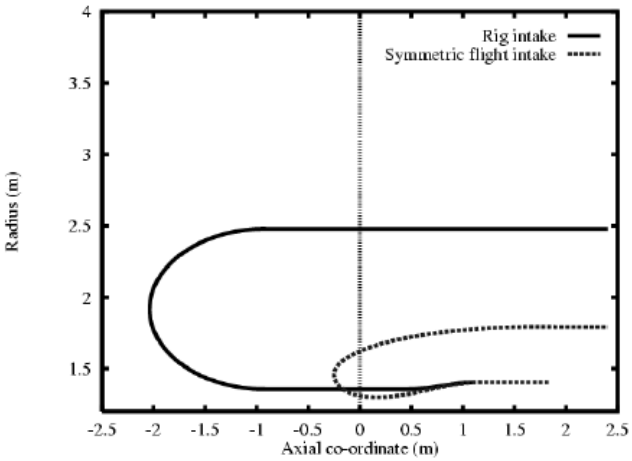

Fig. 1 Flight and rig intakes - Vahdati et al. (2002)

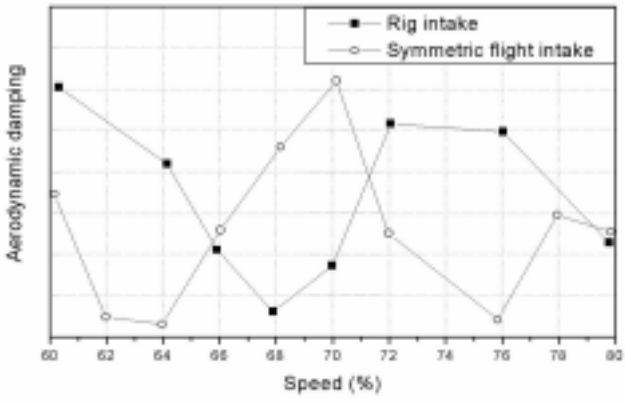

Fig.2 Differences in aerodynamic damping between the two intakes - Vahdati et al. (2002)

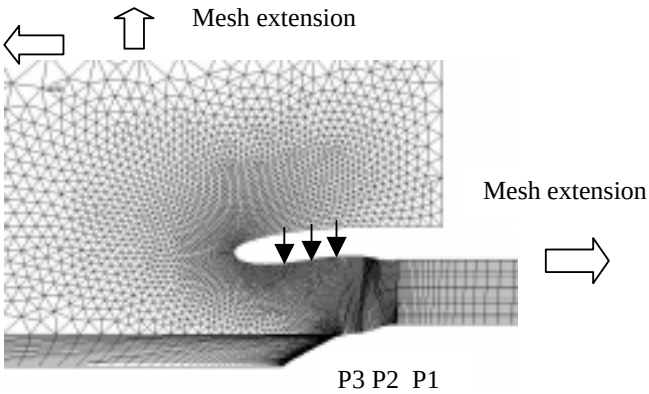

Fig. 3a Periodic boundary grid showing extent of the flow domain

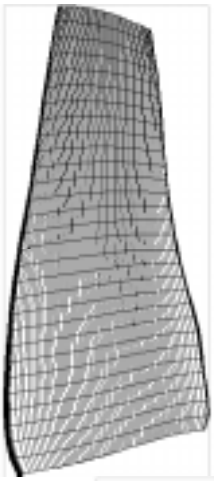

(i)Blade surface

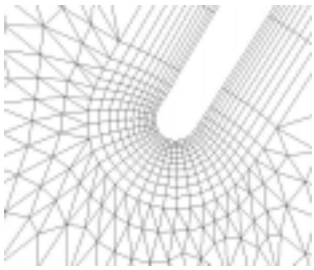

(ii)Leading Edge

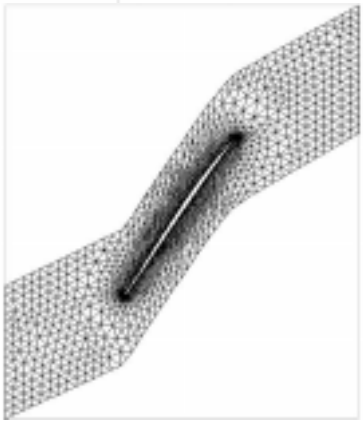

(iii) tip section

Fig. 3b View of the blade mesh

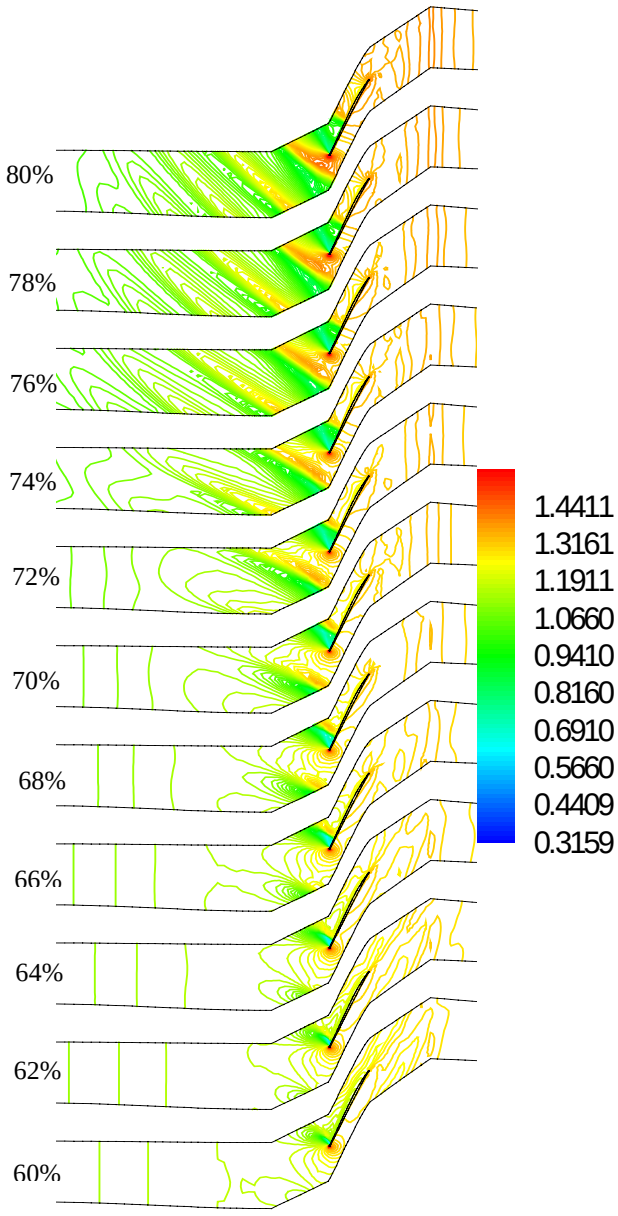

Fig. 4 Steady-state Mach number contours near the blade tip

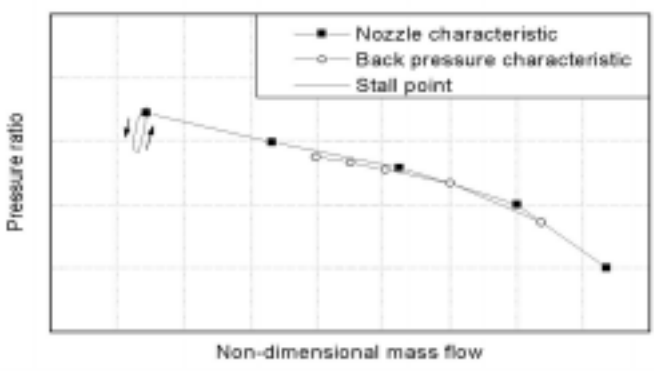

Fig. 5 Determination of stall boundary- Variable nozzle vs fixed back pressure

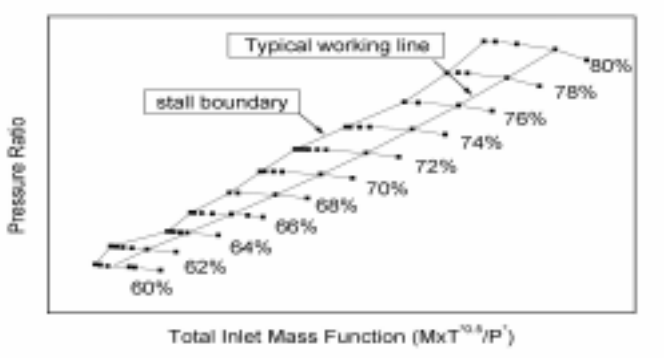

Fig. 6 Mapping of fan characteristic using the variable nozzle method

Fig. 7 Fan blade 1F mode shape

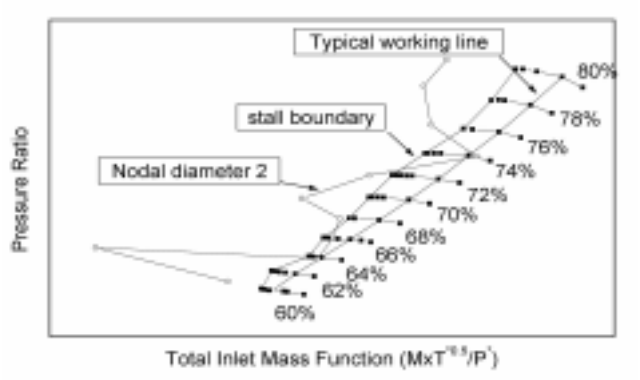

Fig. 8 Determination of flutter bite for 2ND nodal diameter mode

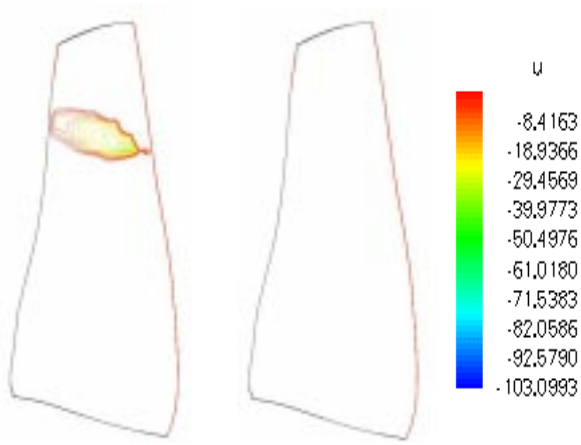

(a) 74% speed (b) 64% speed

Fig. 9 Negative axial velocity at suction surface

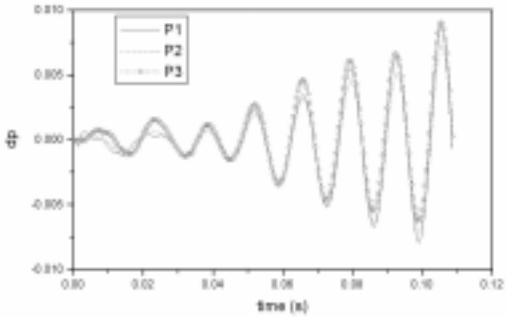

Fig. 10 Pressure (normalized) build-up as the acoustic wave reflects from inside the duct

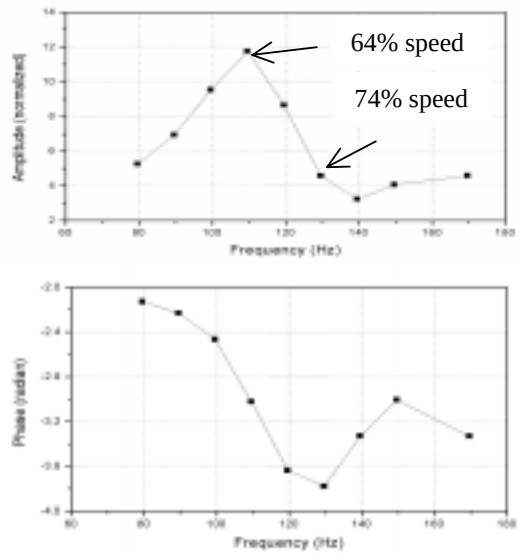

Fig. 11 Duct-alone impedance (Δp/Δu) for 2 nodal diameter pressure perturbation at fan face

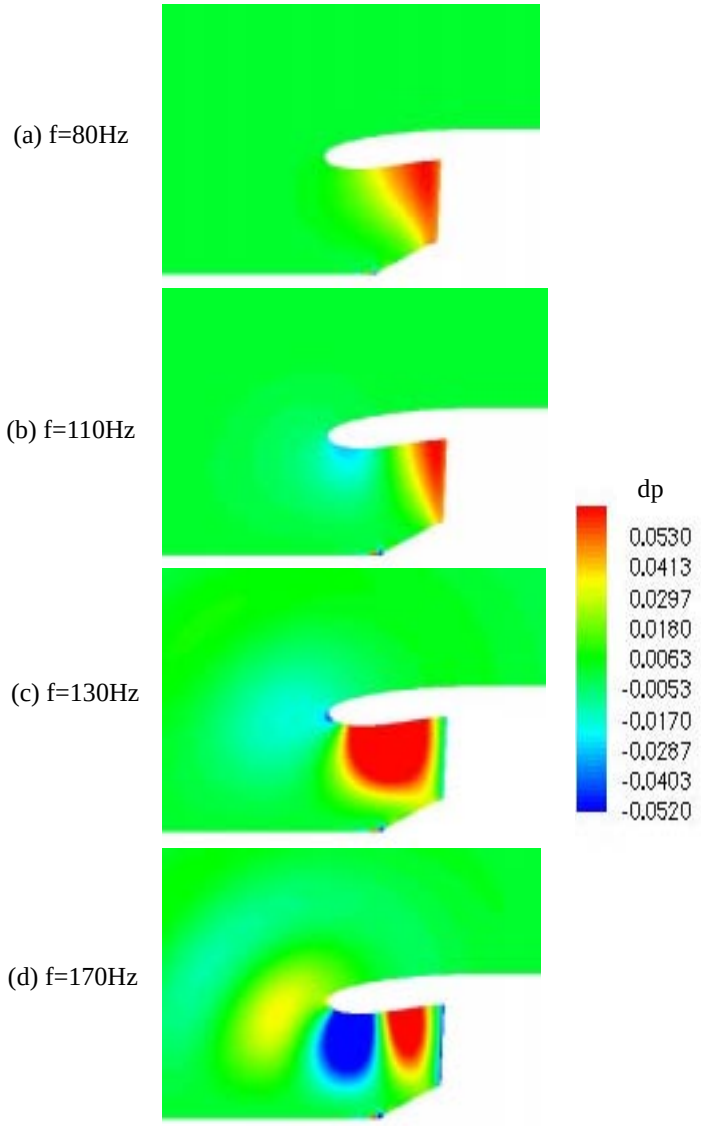

Fig. 12 Pressure contours from duct-alone computations for imposed 2 nodal diameter pressure perturbation at various speeds